CETRA^2026 27-30 May 2026, Bol, Island Brač, Croatia
9th International Conference on Road and Rail Infrastructure

# EXPERIMENTAL AND OPERATIONAL MODAL ANALYSIS ESTIMATION OF DAMPING RATIOS FOR STAYS OF A BRIDGE UNDER CONSTRUCTION

**Roberto Gomez, Marco Mendoza, Raul Sanchez, Martin Arenas, Oscar Rosales**
*Institute of Engineering UNAM, Mexico City, Mexico*

## Abstract

Calculation of damping in cable stayed bridges can be a complicated task because their dynamic response depends on their tension, the boundary conditions generated at their anchorages, and their catenary or geometry. Environmental vibration tests are a well-known and widely used technique to estimate damping ratios, therefore, it is necessary to consider natural frequencies, as well as modal shapes of the cables. In this paper, some techniques of Operational Modal Analysis and signal conditioning were used to derive the dynamic properties of eight cables of a cable-stayed bridge; linear regression models and identification of stochastic state models were used. The results obtained with the experimental applied techniques were compared and the response of the cables to mitigate wind vibrations was assessed based on the capacity of the shock absorbers and the Scruton number.

*Keywords: damping, frequency, cable stayed bridge, operational modal analysis, scruton number*

## 1 Introduction

The cable-stayed bridge includes 7 spans: two spans of 31 m, two spans of 35 m and two spans of 48 m, and a main span of 348 m. The superstructure is made up of 53 steel segments, 12 m long each, while the closing segment is 2 m long; the total width of the deck is 13 m with 7 m of roadway. Figure 1 shows a view of the bridge during the final phase of its construction. A monitoring program was carried out on some of the longest stays using MicroStrain Model G-Link triaxial wireless acceleration sensors with a measurement range of 2g. Stays attached to pylon 4, in a semi-harp array, located on the upstream side were selected, as illustrated in the same figure. In total, 8 stay cables were monitored, 4 located on the main span (6, 9, 11 and 13) and the rest on the opposite side (7, 10, 12 and 14); measurements were taken before and after installing shock absorbers in the anchorage of stays, to improve their damping.

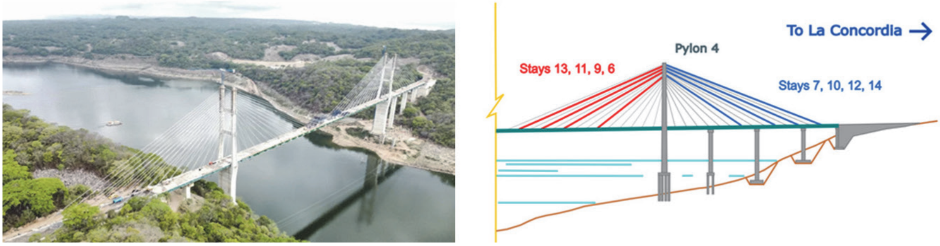


**Figure 1** The Concordia cable stayed bridge (left) and location of the stay cables selected for monitoring (right)

### 1.1 Free vibration testing

Each test carried out consisted of measuring the acceleration in free vibration of each chosen cable. Two measurements were performed per stay cable, therefore, a tension force controlled by an experimental device was provided, which consists of a rope, a winch and a fuse. The latter has the function of providing an impulse that produces the vibration of tie rod once the yield tension has been reached. The magnitude of the acceleration depends on the length and amount of tension produced on the strands that conform each bridge cable. In "Stage 1", the acceleration sensor was placed away from the anchorage, as far/high as possible, without the shock absorber installed. In "Stage 2", the acceleration sensor was placed in the same way, with the shock absorber already installed. During the tests, the asphalt layer and metal railings were placed on the road.

## 2 Analysis and data processing

Damping ratios of a bridge cables can range anywhere from 0.0005 to 0.01, being difficult to predict a precise value. The lower end of this range is typical of very long cable stays without any grout infill, while the upper end of this range is more typical of shorter cable stays with grouting and perhaps some external damping. A realistic estimate of inherent cable damping ratios on service bridges is in the range from 0.001 to 0.005 [1], which also depends on the vibration mode involved. The Logarithmic Decay method is traditionally the most widely used and simple to implement. It is evaluated by selecting successive peaks of the response of a one degree of freedom system in free vibration with little damping ratios or $0 < \xi < 1$, and adjusting their values by an enveloping function that describes the decay rate of the vibration amplitude [2]. In the last decades, other methods have been developed and tested on civil structures to obtain the dynamic characteristics of a structural system. Therefore, the analysis was complemented by the application of some Operational Modal Analysis (OMA) techniques, which allow estimating the modal properties (natural frequencies, modal shapes and damping ratios) from the recorded accelerations from ambient vibration sources obtained during the service stage of a structure [3, 4]. Unlike Experimental Modal Analysis (EMA) techniques, where vibration generators or impact hammers are used, where it is necessary to measure the excitation source [5].
In this paper, in order to correlate the measurements carried out in each stay cable, the modal frequency is obtained by the simple single degree of freedom peak-picking method [6]. It was used to identify the natural vibration frequencies of the first two vibration modes of the cables, then the damping ratios were calculated with the traditional Logarithmic Decrement method applied directly to the time series. Furthermore, the Stochastic Subspace Identification method was applied using its two variants: the first calculates the covariance matrix (SSI-COV), whereas the second applies a projection of the line space of future data on the line space of past data, which is why it is known as the data-based method (SSI-DATA) [3-5, 7, 8].

## 2.1 Logarithmic decrement method

The theory of structural dynamics shows that the solution of the differential equation of motion for the case of free vibration, includes a term that describes the progressive reduction of amplitude of the initial response of a structure, according to equation (1) [9].

$$x(t) = Xe^{-\xi\omega t} = Xe^{-\xi 2\pi f t} \tag{1}$$

Therefore, the calculation of the critical damping ratio is reduced to determining the value of the amplitude "X" and the exponent "-ξω" that best fits the experimental data "x(t)" measured on site. It is necessary to know the vibration frequency "f", therefore the most common method is to perform an analysis in the frequency domain by calculating the fast Fourier transform [10]. Each signal is filtered in relation to the identified frequencies by a band-pass filter of "n" order, which is selected in such a way that the signal is free from the contribution of lower or higher modes; sometimes this is not possible without distorting the signal significantly. Once this has been done, the calculation of the curve that best suits the experimental data and the least squares method is applied to equation (1) to find the best fitting curve. For the calculation of the critical damping ratio, this value is solved according to equation (2):

$$\xi = \frac{-Z}{2\pi f} \tag{2}$$

where "Z" is the exponent of the function that fits the experimental data. Figure 2 shows the method applied to the acceleration time-history measured on Stay 6, where shows the acceleration measured on the test, the frequency domain response and the acceleration of the first two vibration modes filtered with the amplitude envelope. In this case the second mode was not exited because the acceleration sensor was installed near of a node. Therefore, the amplitude of the second mode in the spectral density function is almost zero and the time-history of the acceleration for the second mode is not appropriate to calculate the signal decay.

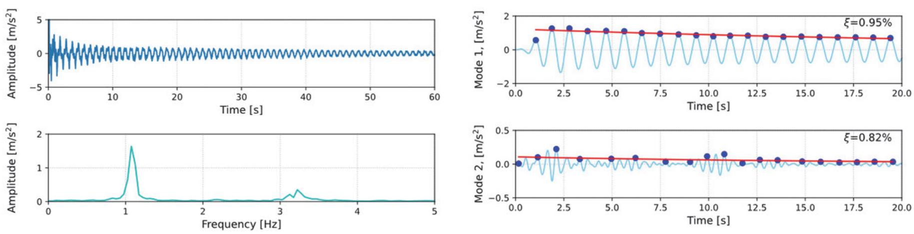


**Figure 2** Acceleration time-history, Stage 1, Stay 6, direction V

## 2.2 Stochastic subspace identification (SSI) method

This method was developed for the design and analysis of control systems [3, 11]. The dynamic response of a continuous mechanical system can be described by the differential equation of motion [12, 13], equation (3) is considered:

$$M\ddot{q}(t) + C_2\dot{q}(t) + Kq(t) = f(t) \tag{3}$$

where "M" is the mass matrix, "C2" is the damping matrix, "K" is the stiffness matrix, "f(t)" is the force, and "q(t)" is the displacement.

Although the above equation represents the dynamic behaviour of a structure, usually is not used directly in system identification methods. For this reason, the equilibrium equation is converted into a time-discretized stochastic space model by equation (4):

$$\begin{aligned} x_{k+1} &= Ax_k + w_k \\ y_k &= Cx_k + v_k \end{aligned} \tag{4}$$

where "k" is the observed instant of time, "$y_k$" ε $R^l$ is the vector containing the measured data, "$x_k$" ε $R^n$ is the discrete state vector and "$w_k$" is the noise vector due to model inaccuracies and "$v_k$" is the noise contained in the measurement, "A" ε $R^{nxn}$ is the state transition matrix and "C" ε $R^{rxn}$ is the observation matrix ("l" is the number of accelerometers and "n" is the order of the system). The modal parameters are calculated by performing the decomposition into singular values SVD of the matrix "A" as proposed in equation (5).

$$A = \Psi \Lambda_d \Psi^{-1} \tag{5}$$

where "Ψ" is the eigenvector matrix and "$\Lambda_d$" is the diagonal matrix containing the eigen-time-discrete values "$\mu_i$" The eigenfrequencies "$\omega_i$" and damping ratios "$\xi_i$" can be calculated from the eigenvalues of the matrix "$\Lambda_d$" considering that "$\Delta_t$" is the sampling time as stated in equations (6)-(7):

$$\mu_i = e^{\lambda_i \Delta t} \tag{6}$$

$$\lambda_i, \lambda_i^* = -\xi_i \omega_i \pm j\sqrt{1 - \xi_i^2}\,\omega_i \tag{7}$$

And finally, the modal shapes "V" can be obtained by multiplying the observation matrix by the eigenvector matrix as shown in equation (8).

$$V = C\Psi \tag{8}$$

The purpose of the SSI method is to find the values of the matrices "A" and "C" describing the behaviour of the system. Therefore, the SSI-COV and the SSI-DATA methods were used to determine these values and their stabilization diagrams were calculated as described below.

## 2.3 Stabilization diagrams

According to the above, the SSI is a mathematical parametric method that it fits to the time data series measured. Proper parameter configuration requires some prior knowledge about the system order to identify the number of modes in the analyzed frequency range. Consequently, this value must be estimated in advance based on a physical perspective or peaks in the output power spectra. The order of the model can be theoretically determined from experimental data such as the range of the Toeplitz matrix of correlations for the SSI-COV method or the Projection matrix for the SSI-DATA method [3, 4, 7]. Figure 3 show an example applied to the data measured and the evolution of the poles for increasing model orders. Physical modes can be identified from stable pole alignments (green dots), as spurious mathematical poles (red dots) tend to be more dispersed and typically do not stabilize. Stable pole alignments can start at values lower or higher than the model order, depending on the excitation level of the modes. The construction of the stabilization diagram is based on the comparison of the poles associated with a given model order with those obtained from a model of a lower order.

Only poles that meet the assigned user-defined stabilization criteria are labelled as stable. Typical stability requirements are expressed by the following inequalities, equations (9)-(10) [7]:

$$\left(\frac{|f(n)-f(n+1)|}{f(n)}\right)<0.01 \tag{9}$$

$$\left(\frac{|\xi(n)-\xi(n+1)|}{\xi(n)}\right)<0.05 \tag{10}$$

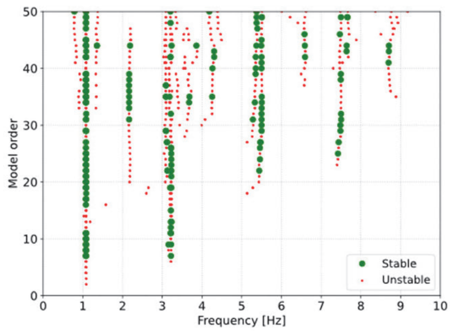


**Figure 3** Stabilization Diagram Stage 1, Stay 6, Direction V, SSI-COV (left), SSI-DATA (right)

If all the conditions expressed by the above inequalities are complied, the pole is labelled as stable [7]. The presence of the damper did not modify the frequency response of the stays, therefore, the observed damping ratios remained practically the same, however, a slight increase in the stay 12 could be seen in the fundamental vibration mode. The graphs in figures 4 and 5 shows a comparison of the damping ratios.

## 3 Comparison of results

The presence of the damper did not modify the frequency response of the stays, therefore, the observed damping ratios remained practically the same, however, a slight increase in the stay 12 could be seen in the fundamental vibration mode. The graphs in figure 4 shows a comparison of the damping ratios obtained for the vibration mode 1 of the stays without damper (stage 1) and with damper (stage 2), and figure 5 shows the same comparison but for vibration mode 2.

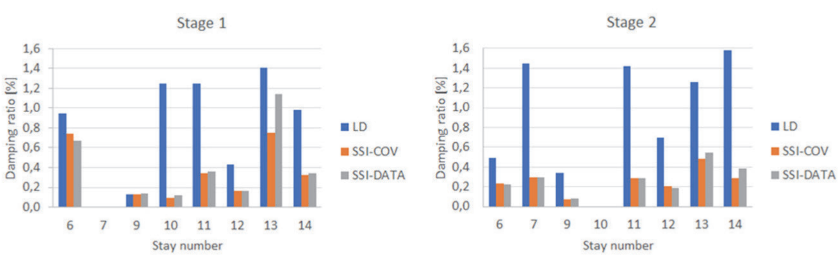


**Figure 4** Comparison of the damping obtained in stage 1 and stage 2, for each stay, mode 1

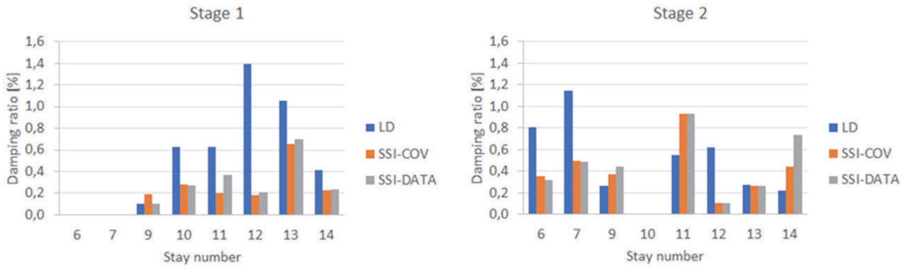


**Figure 5** Comparison of the damping obtained in stage 1 and stage 2, for each stay, mode 2

Figure 4 shows that stay 7 was not measured during stage 1 of testing and stay 10 was not measured during stage 2. Figure 5 shows that the damping ratio of stay 6 was not calculated because mode 2 was not excited (as shown in figure 2) and stay 10 was not measured in stage 2. Both the SSI-COV method and the SSI-DATA method offer similar results unlike the conventional Logarithmic Decay method (LD), which apparently overestimates the damping ratios. This is mainly due to the fact that in this method the presence of other vibration modes usually influences the magnitude of the vibration amplitudes as mentioned by Magalhães [8], in addition to the fact that the choice of the order of the filter used in the filtering of the signals can distort the acceleration time series.

## 3.1 Stability criterion

Cable-stayed bridges around the world commonly present unexpected and excessive vibrations in the cables. Such high-amplitude vibrations induce stress and fatigue in the cables as well as in the anchorages of pylons and superstructure [14]. The Scruton number measures the influence of the damping ratio on the structural response when considering excitation due to vortices, vibrations induced by rain or wind, it is calculated according to equation (11).

$$S_c = \frac{m\xi}{\rho D^2} \tag{11}$$

where "m" is the mass of cable per unit length, "ξ" is the damping ratio, "ρ" is the air density, and "D" is the cable diameter. Most types of wind-induced oscillation tend to be mitigated increasing the Scruton number as high as possible by providing external dampers and/or crossties. Based on the results of Saito, the oscillations caused by the rain-wind interaction can be considered acceptable considering the following criterion [1, 15]: $m\xi/\rho D^2 > 10$ for regular cable arrangements; $m\xi/\rho D^2 > 5$ for cable pipes with effective surface treatment suppressing rain/wind-induced vibrations. A damper can be tuned to yield optimal damping in any one selected mode. For other modes the level of damping will be less than this optimal value. Rain/wind-induced vibrations occur predominantly in mode 2. Therefore, if a damper is to be tuned to a particular mode to mitigate rain/wind-induced vibrations, it appears logical to select mode 2 [1]. Therefore, Scruton number was calculated from the damping ratios obtained experimentally with the SSI-COV method and the second vibration mode of each stay. It was considered that the cables have a regular arrangement and the project data of the studied bridge. The results are showed in the figure 6.

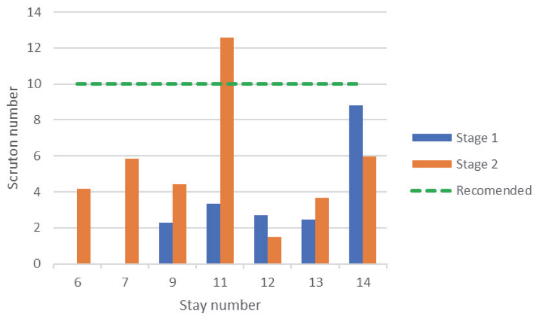


**Figure 6** Scruton numbers calculated from tests in stage 1 and stage 2

### 3.2 Discussion

The mitigation effect of the damper seems to be more consistent with the second mode of vibration in agreement with the experimental data and the expected results for stays 9, 11 and 14 (figure 6). The damper increases the damping ratio and therefore the Scruton number. However, the values do not reach the minimum recommended value so this value must be greater than 10. The differences observed between the calculation methods used consist in that for the decay method the first 20 seconds of the acceleration time history were used. The signal decay fitting is complicated by the sudden changes in the acceleration amplitude in some measurements. Whereas in the other methods (SSI-COV and SSI-Data) the complete record was used. Due to this and the influence of nearby vibration modes, the results can vary significantly as discussed in [8]. By using the entire signal, information is obtained from the interval in free vibration and from the remaining interval in ambient vibration, which is more representative.

## 4 Conclusion

The typical damping interval for cable-stayed bridges is in the range of 0.1 to 0.5% and depend on the vibration mode involved. When comparing the frequency values measured in the stay cables during the two monitoring stages, it is observed that the frequencies of the cables remain unchanged. However, no noticeable difference in wind-generated vibration dissipation was observed at instrumented sites far from the anchors. Scruton numbers calculated with experimental damping ratios indicate that cables may have wind vibration problems when values below 10 are obtained. The experimental data did not show that the damper increased the damping of the stays to dissipate wind vibrations, however other measurements made with the sensors adjacent to the anchors showed that the stays vibration was mitigated completely during the forced vibration tests, which indicates that the sensors were effective in isolating the vibration of the stays in the deck. This helps to reduce fatigue effects on the anchors and consequently increase the useful life of the structure. It is worth clarifying that the measurements were carried out during the construction stage, so the stay cables were not fully tensioned with the design final stresses. Tensioning work was still pending to level the superstructure, so the frequency values and, therefore, the damping ratios presented are not definitive.

## References


[1] Kumarasena, S., Jones, N.P., Irwin, P., Taylor, P.: Wind induced vibration of stay cables, McLean, VA: HNTB Corporation: Federal Highway Administration, 2007.

[2] Casiano, M.J.: Extracting damping ratio from dynamic data and numerical solutions. Huntsville, Alabama: NASA George C. Marshall Space Flight Center, 2016.

[3] Peeters, B., De Roeck, G.: Reference-based stochastic subspace identification for output-only modal analysis, Mech Syst Signal Process, 1999.

[4] Brincker, R., Zhang, L., Andersen, P.: Modal identification of output-only systems using frequency domain decomposition, Smart materials and structures, 10 (2001) 3, pp. 441-445, DOI: 10.1088/0964-1726/10/3/303

[5] Avitabile, P.: Modal Testing: A Practitioner's Guide, USA: Wiley & Sons Ltd, 2018.

[6] Chauhan, S., et al.: Application of OMA-EMIF algorithm to cable stayed bridges, International conference on noise and vibration engineering ISMA2008, Leuven, Belgium, 15-17.09.2008.

[7] Rainieri, C., Fabbrocino, G.: Operational modal analysis of civil engineering structures, New York Springer, 2014.

[8] Magalhães, F., Brincker, R., Cunha, Á.: Damping estimation using free Decays and ambient vibration tests, 2nd International Operational Modal Analysis, pp. 513-521, Copenhagen, Denmark, 30. April-02.May 2007.

[9] Tedesco, J.W., McDougal, W.G., Ross, A.C.: Structural Dynamics Theory and applications, Menlo Park, Calif. Adison Wesley Longman, 1999.

[10] Bendat, J.S., Piersol, A.G.: Random data: analysis and measurements procedures, New York Wiley Interscience, 1989.

[11] Viberg, M.: Subspace methods in system identification, IFAC System identification Copenhagen Denmark, 1994.

[12] Peeters, B., De Roeck, G.: Stochastic system identification for operational modal analysis: A review, Journal of dynamic systems measurement and control, 2001.

[13] Lengvarsky, P., Bocko, J.: Theoretical basis of modal analysis, American journal of mechanical engineering, 2013., pp. 173-179

[14] Jones, N.P., Main, J.: Stay cable vibration measurements, mechanisms and mitigation, 1998.

[15] Zhou, S., Yunfeng, Z., Xugang, H., Fanrong, X., Xuandong, L.: Investigation of the Scruton number effects of wind-induced unsteady galloping responses of bridge suspenders, Shock and vibration, 2021.